FASTC-ID(RS)T-0867-92

# FOREIGN AEROSPACE SCIENCE AND TECHNOLOGY CENTER


NUMERICAL COMPUTATION OF INVISCID FLOW AROUND NOSE TIP OF SPACE SHUTTLE WITH NND SCHEME

by

Ye Youda, Guo Zhiquan, et al.

# HUMAN TRANSLATION

FASTC-ID(RS)T-0867-92 27 April 1993

MICROFICHE NR: 93C000299

NUMERICAL COMPUTATION OF INVISCID FLOW AROUND NOSE TIP OF SPACE SHUTTLE WITH NND SCHEME

By: Ye Youda, Guo Zhiquan, et al.

English pages: 14

Source: Unknown; pp. 282-290

Country of origin: China
Translated by: Leo Kanner Associates
F33657-88-D-2188
Requester: FASTC/TATV/Capt Stephen W. Stiglich, Jr.
Approved for public release; Distribution unlimited.





PREPARED BY:

TRANSLATION DIVISION
FOREIGN AEROSPACE SCIENCE AND TECHNOLOGY CENTER
WPAFB, OHIO

GRAPHICS DISCLAIMER

All figures, graphics, tables, equations, etc. merged into this translation were extracted from the best quality copy available.

# NUMERICAL COMPUTATION OF INVISCID FLOW AROUND NOSE TIP OF SPACE SHUTTLE WITH NND SCHEME

**ABSTRACT:** The NND scheme presented by Professor Zhang Hanxin of the CARDC has been used in this paper to complete the following computations: the two-dimensional inviscid flow around the symmetric plane of the nose tip of the space shuttle; the three-dimensional inviscid flow around the nose tip of the space shuttle; the three dimensional inviscid flow around the axisymmetric indented body. Under the general coordinate system, the computation grids have been generated by algebra equations. The characteristic compatibility equations have been used to treat the shock and body surface boundaries, and there is a special treatment in translation of the coordinate system. Finally, the comparative computations have been completed using second order SCM schemes. The results of computation illustrate that the NND scheme used in this paper can avoid numerical oscillations and high resolution to shock-capturing.

Since J.V. Rakich[1/] used MacCormack two step grid computation of the space shuttle flow field, several people [2-7/] have done work in this area. For the mixed zones of the nose cone, the stabilization method was used. For the super sonic areas of the body of the space craft, the propulsion method was used. For the external shock wave, an assembly method was used. These methods are the general methods for such complex shapes as a space shuttle. However, engineers have always been searching for a simple calculation method with a small amount of computation which is deeply rooted in physics.

In 1983, A. Harten proposed a total variation decrease scheme[8/]. This scheme is very effective in capturing the shock wave and can also eliminate the normal two step scheme for capturing the vibration generated when capturing the shock wave. Later, this scheme based on the idea of flux limitation was widely

expanded[9-18]. In 1985, H.C. Yee used the TVD scheme to do computations for the NACA 0012 wing form on a graphic coordinate system, and S.R. Chakravarthy applied the TVD scheme to computations for complex shapes, both with good results.

Last year, at the discussion section on "The TVD Scheme and Its Applications" held by the graduate department at the Aerodynamics Research Center, Professor Zhang Hanxin proposed a NND scheme which, when compared to other TVD schemes, has the advantage of being simple and having a small amount of computations. This article will use this NND scheme to compute the two dimensional inviscid flow around the symmetrical cross section of the nose tip of the space shuttle and the three dimensional inviscid flow around the nose tip of the space shuttle and the axisymmetric indented body. The results indicate that it is satisfactory for both the scheme convergence speed and the capture of the shock wave within the flow field.

## II: CONTROL FORMULA AND BOUNDARY CONDITIONS

### 1. CONTROL FORMULA

For a rectangular coordinate system, Euler's formula may be written:

$$\frac{\partial U}{\partial t} + \frac{\partial E}{\partial x} + \frac{\partial F}{\partial y} + \frac{\partial G}{\partial z} = 0$$

In this formula:

$$U = \begin{bmatrix} e \\ \rho \\ \rho u \\ \rho v \\ \rho w \end{bmatrix} \qquad E = \begin{bmatrix} (e+p)u \\ \rho u \\ \rho u^2 + p \\ \rho uv \\ \rho uw \end{bmatrix}$$

$$F = \begin{bmatrix} (e+p)v \\ \rho v \\ \rho uv \\ \rho v^2 + p \\ \rho vw \end{bmatrix} \qquad G = \begin{bmatrix} (e+p)w \\ \rho w \\ \rho uw \\ \rho vw \\ \rho w^2 + p \end{bmatrix}$$

$$e = \frac{p}{\gamma - 1} + \frac{\rho}{2}(u^2 + v^2 + w^2)$$

Converting:

$$\begin{cases} t = \tau \\ \xi = \xi(t, x, y, z) \\ \eta = \eta(t, x, y, z) \\ \zeta = \zeta(t, x, y, z) \end{cases}$$

We obtain the control formula for the object surface coordinates:

$$\frac{\partial \tilde{U}}{\partial \tau} + \frac{\partial \tilde{E}}{\partial \xi} + \frac{\partial \tilde{F}}{\partial \eta} + \frac{\partial \tilde{G}}{\partial \zeta} = 0$$

In this formula:

$$\tilde{U} = U / J$$
$$\tilde{E} = (\xi_t U + \xi_x E + \xi_y F + \xi_z G) / J$$
$$\tilde{F} = (\eta_t U + \eta_x E + \eta_y F + \eta_z G) / J$$
$$\tilde{G} = (\zeta_t U + \zeta_x E + \zeta_y F + \zeta_z G) / J$$
$$J = \frac{\partial(\xi, \eta, \zeta)}{\partial(x, y, z)}$$

If:

$$\tilde{A} = \frac{\partial \tilde{E}}{\partial \tilde{U}}, \quad \tilde{B} = \frac{\partial \tilde{F}}{\partial \tilde{U}}, \quad \tilde{C} = \frac{\partial \tilde{G}}{\partial \tilde{U}}$$

Then $\tilde{A}$, $\tilde{B}$, $\tilde{C}$ have the characteristic values of:

$$\begin{cases} \lambda_1 = n_t + n_x u + n_y v + n_z w - C\sqrt{n_x^2 + n_y^2 + n_z^2} \\ \lambda_2 = n_t + n_x u + n_y v + n_z w \\ \lambda_3 = n_t + n_x u + n_y v + n_z w + C\sqrt{n_x^2 + n_y^2 + n_z^2} \end{cases}$$

n represents $\xi$ , $\eta$ , or $\zeta$ .

## 2. BOUNDARY CONDITIONS

On the surface of an object, ( $\eta=0$ ), a condition for impermeability:

On a shock wave surface, ( $\eta=1.0$ ), using the R-H relationship in a movement coordinate system, we can obtain:

$$\vec{U}_\infty = u_\infty \vec{i} + v_\infty \vec{j} + w_\infty \vec{k}$$

$$\vec{N}_s = (\eta_x \vec{i} + \eta_y \vec{j} + \eta_z \vec{k}) / \sqrt{\eta_x^2 + \eta_y^2 + \eta_z^2}$$

$$\mu = \mathrm{sign}(\vec{U}_\infty \cdot \vec{N}_s)$$

$$M_s = \left[ \frac{\gamma+1}{2\gamma} \left( \frac{p_2}{p_\infty} - \frac{\gamma-1}{\gamma+1} \right) \right]^{1/2}$$

$$V_{\infty N} = (\vec{U}_\infty \cdot \vec{N}_s)\,\mu$$

$$V_s = \frac{M_s}{M_\infty} - V_{\infty N}$$

$$\vec{V}_s = -\mu V_s \vec{N}_s$$

$$V_{2N} - V_{\infty N} = \frac{2(1-M_s^2)}{(\gamma+1) M_s M_\infty}$$

$$\rho_s = \left( \frac{p_2}{p_\infty} + \frac{\gamma-1}{\gamma+1} \right) \Big/ \left( 1 + \frac{\gamma-1}{\gamma+1} \frac{p_2}{p_\infty} \right)$$

$$\vec{V}_2 = \vec{U}_\infty + \mu (V_{2N} - V_{\infty N}) \vec{N}_s$$

Herein, the subscript "2" represents the post wave value and N is the vector of the front of the shock wave.

# III: DIFFERENCE SCHEME AND BOUNDARY PROCESSING

## 1. DIFFERENCE SCHEME

This article uses the non division explicit difference scheme

$$\tilde{U}_{i,j,k}^{n+1} = \tilde{U}_{i,j,k}^{n} - \lambda_\xi (\tilde{E}_{i+\frac{1}{2},j,k} - \tilde{E}_{i-\frac{1}{2},j,k})$$

$$- \lambda_\eta (\tilde{F}_{i,j+\frac{1}{2},k} - \tilde{F}_{i,j-\frac{1}{2},k}) - \lambda_\zeta (\tilde{G}_{i,j,k+\frac{1}{2}} - \tilde{G}_{i,j,k-\frac{1}{2}})$$

Herein:

$$\lambda_\xi=-\frac{\Delta t}{\Delta\xi},\quad \lambda_\eta=\frac{\Delta t}{\Delta\eta},\quad \lambda_\zeta=-\frac{\Delta t}{\Delta\zeta}$$

$$\tilde{E}_{i+\frac{1}{2},j,k}=\tilde{E}^{+}_{i+\frac{1}{2},j,k}+\tilde{E}^{-}_{i+\frac{1}{2},j,k}$$

$$\tilde{E}^{+}_{i+\frac{1}{2},j,k}=\tilde{E}^{+}_{i,j,k}+\frac{1}{2}\,\mathrm{minmod}(\Delta\tilde{E}^{+}_{i-\frac{1}{2},j,k},\ \Delta\tilde{E}^{+}_{i+\frac{1}{2},j,k})$$

$$\tilde{E}^{-}_{i+\frac{1}{2},j,k}=\tilde{E}^{-}_{i+1,j,k}-\frac{1}{2}\,\mathrm{minmod}(\Delta\tilde{E}^{-}_{i+\frac{3}{2},j,k},\ \Delta\tilde{E}^{-}_{i+\frac{1}{2},j,k})$$

$$\Delta\tilde{E}^{\pm}_{i+\frac{1}{2},j,k}=\tilde{E}^{\pm}_{i+1,j,k}-\tilde{E}^{\pm}_{i,j,k}$$

$$\tilde{E}^{\pm}_{i,j,k}=R_{i,j,k}\Lambda^{\pm}_{i,j,k}L_{i,j,k}\tilde{U}$$

$$\Lambda^{\pm}_{i,j,k}=\frac{1}{2}(\Lambda_{i,j,k}\pm|\Lambda_{i,j,k}|)$$

$$\Lambda=\mathrm{diag}(\lambda_1,\ \lambda_2,\ \lambda_3,\ \lambda_4,\ \lambda_5)$$

A similar expression can also be written for $\tilde{F}_{i,j+\frac{1}{2},k}$, $\tilde{G}_{i,j,k+\frac{1}{2}}$

$$\mathrm{minmod}(x,\ y)=\begin{cases}0 & xy<0\\ x & |x|\le|y|\\ y & |x|>|y|\end{cases}$$

which are called limiting factors.

## 2. BOUNDARY PROCESSING

Because the boundary conditions of the physical object and the boundary conditions of the shock wave are incomplete, it is necessary to have four additional formulas for the surface of the object and one additional formula for the shock wave. According to characteristic theory, in fluid motion, the information is broadcast along a characteristic direction. On a shock wave, there is a characteristic direction orientated with the shock wave. The formula for its consistent relationships can be used to supplement shock wave conditions. On the surface of the object, there are four characteristic consistent relationship formulas which can be used to supplement object surface conditions. In this manner, the object surface and the shock wave boundary formulas are confined.

On the shock wave, $\lambda_5>0$. Its consistent relationship formula can be written as:

$$\sum_{i=1}^{5} l_{5i}\left(\frac{\partial U_i}{\partial \tau}+\sum_{j=1}^{5} l_{ij}\lambda_j\frac{\partial U_j}{\partial \eta}+\tilde{H}_i\right)=0$$

$$\tilde{H}=\tilde{A}\frac{\partial U}{\partial \xi}+\tilde{C}\frac{\partial U}{\partial \zeta}$$

By collating we obtain:

$$\frac{1}{\sqrt{2}}\left(\frac{1}{\rho c}-\frac{\rho M_2}{2}\left(\frac{1-M_2^2}{M_2^2}\right)\right)\frac{\partial p}{\partial \tau}=-\sum_{i=1}^{5} l_{5i}\left(\lambda_i\frac{\partial U_i}{\partial \eta}+\tilde{H}_i\right)$$

After we obtain the post wave pressure p2, we insert it into the shock wave boundary conditions, and we an obtain other post wave parameters.

Because the object surface is static, the impermeable conditions can be written as:

$$\hat{\eta}_x\frac{\partial u}{\partial \tau}+\hat{\eta}_y\frac{\partial v}{\partial \tau}+\hat{\eta}_z\frac{\partial w}{\partial \tau}=0$$

On the object surface, $\lambda_5>0$. Its characteristic consistent relationship formula is substituted for by the object surface impermeable conditions. After insertion into the impermeable conditions, the object surface value boundary conditions are:

$$D\frac{\partial U}{\partial \tau}+\tilde{R}+\tilde{S}=0$$

Herein

$$D=\begin{bmatrix} l_{11} & l_{12} & l_{13} & l_{14} & l_{15} \\ l_{21} & l_{22} & l_{23} & l_{24} & l_{25} \\ l_{31} & l_{32} & l_{33} & l_{34} & l_{35} \\ l_{41} & l_{42} & l_{43} & l_{44} & l_{45} \\ 0 & 0 & \hat{\eta}_x & \hat{\eta}_y & \hat{\eta}_z \end{bmatrix}$$

$$\tilde{R}=\begin{bmatrix} \lambda_1\sum l_{1i}U_{i\eta} \\ \lambda_2\sum l_{2i}U_{i\eta} \\ \lambda_3\sum l_{3i}U_{i\eta} \\ \lambda_4\sum l_{4i}U_{i\eta} \\ 0 \end{bmatrix}=\begin{bmatrix} R_1 \\ R_2 \\ R_3 \\ R_4 \\ 0 \end{bmatrix}$$

$$\tilde{S} = \begin{bmatrix} \Sigma l_{1,} \tilde{H}_{i} \\ \Sigma l_{2,} \tilde{H}_{i} \\ \Sigma l_{3,} \tilde{H}_{i} \\ \Sigma l_{4,} \tilde{H}_{i} \\ 0 \end{bmatrix} = \begin{bmatrix} S_1 \\ S_2 \\ S_3 \\ S_4 \\ 0 \end{bmatrix}$$

Subscript ij a vector matrix element of the $\tilde{B}$ left characteristic matrix.

By collating lambda, we obtain:

$$\frac{\partial p}{\partial \tau} = -\sqrt{2}\, C(R_1 - S_1)$$

$$\frac{\partial \rho}{\partial \tau} = -\frac{1}{\sqrt{2}}\left[\sqrt{2}(R_1 - S_1) + \hat{\eta}_x(R_2 + S_2) + \hat{\eta}_y(R_3 - S_3) + \hat{\eta}_z(R_4 - S_4)\right]$$

$$\frac{\partial u}{\partial \tau} = \frac{1}{\rho}\left[\hat{\eta}_x(R_1 - S_1) - \hat{\eta}_z(R_3 + S_3)\right]$$

$$\frac{\partial v}{\partial \tau} = \frac{1}{\rho}\left[\hat{\eta}_y(R_4 + S_4) - \hat{\eta}_x(R_2 + S_2)\right]$$

$$\frac{\partial w}{\partial \tau} = \frac{1}{\rho}\left[\hat{\eta}_z(R_3 + S_3) - \hat{\eta}_y(R_4 - S_4)\right] \qquad \hat{\eta}_{x,y,z} = \eta_{x,y,z} / \sqrt{\eta_x^2 + \eta_y^2 + \eta_z^2}$$

From the formulas above we can obtain the object surface physics quantities.

At the object axial boundary, using span axial series differential equations we can avoid the irregularities produced by three dimensional coordinate conversion. For symmetric surfaces, we use symmetry to carry out parameter extrapolation of the supplementary boundary values.

## IV: COMPUTATION EXAMPLES

### 1. TWO DIMENSIONAL

In order to check the stability and convergence rate of the differential scheme as well as the suitability of the boundary processing, this article first applies the scheme to space shuttle nose tip symmetrical cross section two dimensional non viscous flow

computations. In order to speed up the convergence, it uses partial time steps.

$$\Delta t = \frac{\Delta t_{ref}}{|U| + |V| + C\sqrt{\xi_x^2 + \xi_y^2 + \eta_x^2 + \eta_y^2}}$$

In this formula, U and V are velocity along the directions xi and eta. Delta time subscript reference is determined by the numerical test. The graph was 61 by 11, and the initial shock wave form was a parabola.

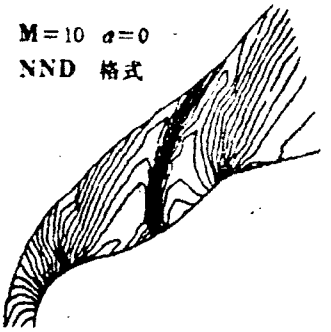


ILLUSTRATION ONE: ISOBARIC CHART (NND SCHEME)

Illustration one is the isobaric chart of the flow field when the angle of attack is zero. Illustration two is a comparison of the pressure on the object surface obtained through computation under conditions of viscous and non viscous flow. Illustration three is a comparison of the computed results using the NND and the SCM schemes. From these illustrations we can see that the NND scheme not only can do a good job in capturing the shock wave in the flow field, but does not generate oscillation near the shock wave. From Illustration two we can see that because of the existence of separated areas, the shock wave in the viscous flow calculations is much weaker that in the non viscous flow. Therefore, changes in object surface pressure tend to be more gradual.

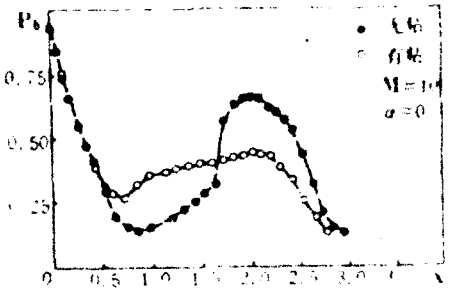

ILLUSTRATION TWO: COMPARISON OF OBJECT SURFACE PRESSURE WITH VISCOUS AND NON VISCOUS FLOW

NOTE: Solid dots are viscous flow, and hollow dots are non viscous.

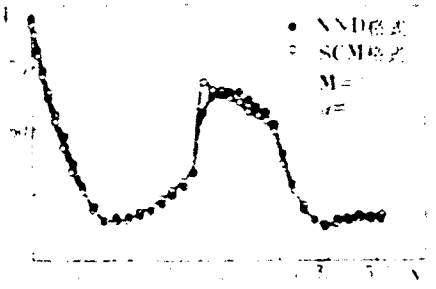

ILLUSTRATION THREE: COMPARISON OF SURFACE PRESSURE DISTRIBUTION

## 2. THREE DIMENSIONAL

Three dimensional computations include two parts, the space shuttle nose tip and the axisymmetric indented body. The Mach number is 10.1 and no consideration is given to yawing. The time step is:

$$\Delta t = CN \times \min\left( \frac{\Delta\xi}{|\lambda_\xi|_{max}} , \frac{\Delta\eta}{|\lambda_\eta|_{max}} , \frac{\Delta\zeta}{|\lambda_\zeta|_{max}} \right)$$

The graph is 41 y 11 by 17. The initial shock wave form is presented as a spiral parabolic surface. The space shuttle nose tip calculated angle of attack was calculated at both 0.0 and minus

5.0 degrees. The indented body calculations were made for both 0.0 and minus 5.0 degrees.

Illustration four is the calculated result of the space shuttle nose tip flow field at an angle of attack of minus 5.0 degrees. Illustration five is the meridian surface pressure distribution calculated with the NND scheme and the SCM scheme compared with as bibliographical item number 19. The results are fairly consistent.

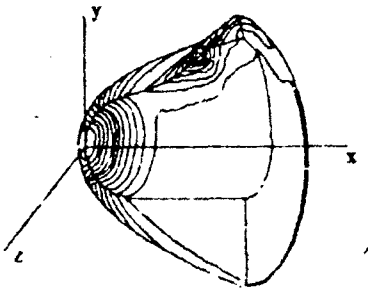


(M = 10, α = -5.0, NND)

ILLUSTRATION ONE
ISOBARS

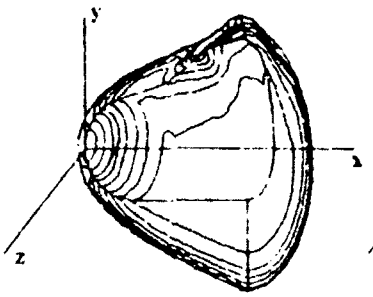


(M = 10, α = -5.0, NND

ILLUSTRATION TWO
ISOPYCNAL

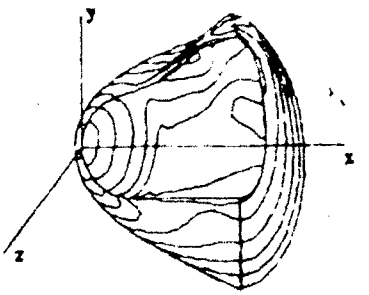


(M = 10, α = -5.0, NND

ILLUSTRATION THREE
ISOMACH

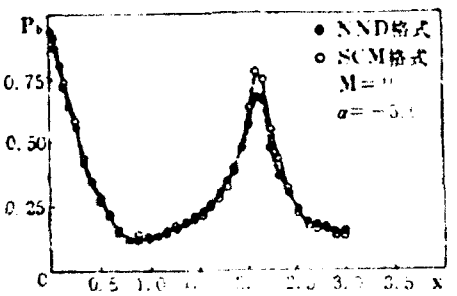


ILLUSTRATION 5.1: COMPARISON OF OBJECT SURFACE PRESSURE DISTRIBUTION

NOTE: Solid dot is NND scheme. Hollow dot is SMC scheme.

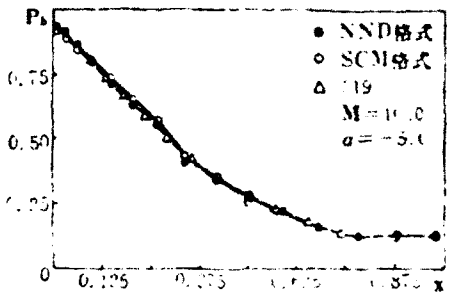


ILLUSTRATION 5.2: COMPARISON OF OBJECT SURFACE PRESSURE DISTRIBUTION

NOTE: Solid dot is NND scheme, hollow dot is SCM scheme.

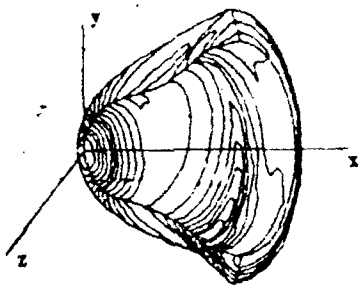


ILLUSTRATION SIX
ISOBARIC GRAPH

Illustration six is an isobaric graph of the indented body flow field at an angle of attack of five degrees. Illustration seven is pi meridian object surface pressure distributions calculated with the NND and SCM schemes compared with bibliographic item 19. The results also conform very well.

ILLUSTRATION 7.1: OBJECT SURFACE PRESSURE DISTRIBUTION COMPARISON

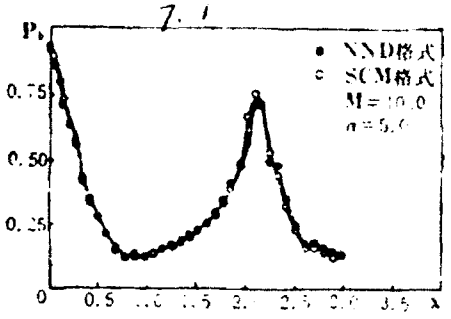


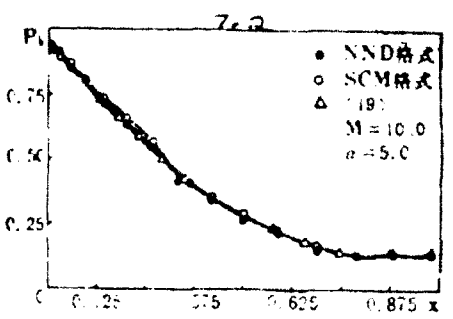


ILLUSTRATION 7.2: OBJECT SURFACE PRESSURE DISTRIBUTION COMPARISON

V: CONCLUSIONS

1. The NND scheme used in this article is not only structurally simple and has a small amount of computations, its results in computing complex forms are also satisfactory.

2. The NND scheme used in this article can do a good job of capturing shock waves in flow fields, it has fairly high discrimination, and it does not create physical vibrations near the shock wave.

3. In the production of a three dimensional graph, this article used span axial series differential equations, thus avoiding irregularities produced by coordinate conversion. and reducing the amount of computation. The computational graph generated using algebra formulas is not only quick with a small amount of computation, but it also is accurate and meets requirements.

## BIBLIOGRAPHY

[1] Rakich, J. V. et al; AIAA 72-191.
[2] Weilmuenster, K. J. et al; AIAA 81-1203.
[3] Rizk, Y. M. et al; AIAA 81-1261.
[4] Venkatapathy, E. et al; AIAA 82-0026.
[5] Prabhu, D. K. et al; AIAA 84-1747.
[6] Rizk, Y. M. et al; AIAA 85-0168.
[7] Chaussee, D. S. et al; NASA TM-85-977.
[8] Harten, A.; J. of Comp. Phys. 49, (1983), 357—393.
[9] Yee, H. C. et al; AIAA 83-1902.
[10] Davis, S. F.; NASA CR-172373.
[11] Yee, H. C.; NASA TM-86842.
[12] Yee, H. C. et al; AIAA 85-1513.
[13] Chakravarthy, S. R.; AIAA 86-0243.
[14] Chakravarthy, S. R. et al, NASA TM-78605.
[15] Chakravarthy, S. R. et al, AIAA 80-0268.
[16] Chakravarthy, S. R. et al, AIAA 83-1943.
[17] Chakravarthy, S. R. et al; AIAA 85-0363.
[18] Chakravarthy, S. R. et al, AIAA 85-1703.
[19] Lyubimov, A. N. et al; NASA-TT-F715, Feb. (1973).
[20]. Zhang Hanxin, TVD Scheme and Its Applications, Aerodynamics Center Journal, (1987).

# DISTRIBUTION LIST

## DISTRIBUTION DIRECT TO RECIPIENT

| ORGANIZATION | MICROFICHE |
|---|---|
| B085 DIA/RTS-2FI | 1 |
| C509 BALLOC509 BALLISTIC RES LAB | 1 |
| C510 R&T LABS/AVEADCOM | 1 |
| C513 ARRADCOM | 1 |
| C535 AVRADCOM/TSARCOM | 1 |
| C539 TRASANA | 1 |
| Q592 FSTC | 4 |
| Q619 MSIC REDSTONE | 1 |
| Q008 NTIC | 1 |
| Q043 AFMIC-IS | 1 |
| E051 HQ USAF/INET | 1 |
| E404 AEDC/DOF | 1 |
| E408 AFWL | 1 |
| E410 ASDIC/IN | 1 |
| E411 ASD/FTD/TTIA | 1 |
| E429 SD/IND | 1 |
| P005 DOE/ISA/DDI | 1 |
| P050 CIA/OCR/ADD/SD | 2 |
| 1051 AFIT/LDE | 1 |
| P090 NSA/CDB | 1 |
| 2206 FSL | 1 |

Microfiche Nbr: FTD93C000299
FTD-ID(RS)T-0867-92